Patient-specific 3D printed pulmonary artery model: A preliminary study

Sultan Aldosari[1], Andrew Squelch[2,3], Zhonghua Sun[1]

1. Department of Medical Radiation Sciences, Curtin University, GPO Box U1987 Perth, Western Australia 6845, Australia
2. Department of Exploration Geophysics, Western Australian School of Mines, Curtin University, GPO Box U1987 Perth, Western Australia 6845, Australia
3. Curtin Institute for Computation, Curtin University, GPO Box U1987 Perth, Western Australia 6845, Australia

Corresponding author:

Professor Zhonghua Sun, Department of Medical Radiation Sciences, Curtin University, GPO Box, U1987, Perth, Western Australia 6845, Australia

Tel: +61-8-9266 7509

Fax: +61-8-9266 2377

Email: z.sun@curtin.edu.au

Abstract

Background and objectives: Three-dimensional (3D) printing has potential value in medical applications with increasing reports in the diagnostic assessment of cardiovascular diseases. The use of 3D printing in replicating pulmonary artery anatomy and diagnosing pulmonary embolism is very limited. The purpose of this study was to develop a 3D printed pulmonary artery model and test different computed tomography (CT) scanning protocols for determination of an optimal protocol with acceptable image quality, but low radiation dose.

Materials and Methods: A patient-specific 3D printed pulmonary artery model was created based on contrast-enhanced CT images in a patient with suspected pulmonary embolism. Different CT pulmonary angiography protocols consisting of 80, 100 and 120 kVp, pitch 0.7, 0.9 and 1.2 with 1 mm slice thickness and 0.6 mm reconstruction interval were tested on the phantom. Quantitative assessment of image quality in terms of signal-to-noise ratio (SNR) was measured in the images acquired with different protocols. Measurements in pulmonary artery diameters were conducted and compared between pre- and post-3D printed images and 3D printed model.

Results: The 3D printed model was found to replicate normal pulmonary artery with high accuracy. The mean difference in diameter measurements was less than 0.8 mm (<0.5% deviation in diameter). There was no significant difference in SNR measured between these CT protocols (p=0.96-0.99). Radiation dose was reduced by 55% and 75% when lowering kVp from 120 to 100 and 80 kVp, without affecting image quality.

Conclusions: It is feasible to produce a 3D printed pulmonary artery model with high accuracy in replicating normal anatomy. Different CT scanning protocols are successfully tested on the model with 80 kVp and pitch 0.9 being the optimal one with resultant diagnostic images but at much lower radiation dose.

Keywords: Diagnosis, image quality, model, pulmonary artery, three-dimensional printing

INTRODUCTION

Three-dimensional (3D) printing is a rapidly developing technique showing increasing interest and great potential in medicine. [1-5] The diagnostic application of using patient-specific 3D printed models has been reported in the diagnostic assessment of cardiovascular disease, pre-surgical planning and simulation, as well as medical education. [6-13] These studies created 3D printed realistic models using either computed tomography (CT) or magnetic resonance imaging (MRI) or echocardiography data with accurate replication of anatomical structures and pathological changes. A recent systematic review of 48 studies has demonstrated the usefulness of 3D printed models in replicating complex cardiovascular anatomy with high accuracy, serving as a valuable tool for pre-surgical planning and simulation of cardiovascular disease, and medical education to healthcare professionals and medical students. [14]

To the best of our knowledge, very few research studies have been conducted in the diagnostic assessment of 3D printed models in pulmonary artery diseases. [15] CT pulmonary angiography (CTPA) is the preferred imaging modality in the diagnosis of pulmonary embolism. [16-20] Although CTPA has high diagnostic value in detecting pulmonary embolism, it has disadvantages of the associated high radiation dose. Further, administration of contrast medium during CTPA represents another limitation with a potential risk of contrast-induced nephropathy. [21, 22] Therefore, reduction of both radiation and contrast medium doses during CTPA is the current research direction with promising results achieved.

According to these studies, there is still potential for further lowering of the radiation and contrast medium doses during CTPA. To test the feasibility of different protocols, a realistic anatomic phantom is an ideal option, and a 3D printed model serves this purpose. Thus, the primary aim of this study was to use a patient-specific 3D printed pulmonary artery model to test different CTPA protocols with the aim of identifying optimal CTPA protocol. Further, potential factors including image segmentation, editing and 3D printing processes could affect the dimensional accuracy of 3D printed models. [23, 24] Witowski et al in their recent systematic review indicates the lack of quantitative methods to validate liver model accuracy. [25] Similarly, no studies have reported the quantitative assessment of 3D printed pulmonary model accuracy. Therefore, the secondary aim of this study was to quantitatively assess the model accuracy of 3D printed pulmonary artery model in delineating anatomical structures.

MATERIALS AND METHODS

Sample image selection

CTPA images from a 53-year-old female with suspected pulmonary embolism were selected in this study to generate 3D reconstructed pulmonary artery model for 3D printing. CTPA showed normal pulmonary artery without any sign of pulmonary embolism. The CT scan was performed on a 128-slice scanner (Siemens Definition Flash, Siemens Healthcare, Forchheim, Germany) with slice thickness of 1.0 mm and reconstruction interval of 0.6 mm.

Image postprocessing and segmentation for 3D printing

Original digital imaging and communications in medicine (DICOM) of CTPA images were transferred to a separate workstation equipped with Analyze 12.0 (AnalyzeDirect, Inc., Lexana, KS, USA) for image processing and segmentation. Semi-automatic approach was used to perform image postprocessing and segmentation of 3D volume data. A CT number thresholding technique was first used to produce 3D volume rendering images with inclusion of the pulmonary trunk, left main and right main pulmonary arteries. In brief, CT attenuation in the pulmonary arteries was measured (around 150 Hounsfield unit [HU]) and applied as the lowest threshold to demonstrate only contrast-enhanced pulmonary arteries and cardiac chambers, while soft tissue, pulmonary veins and other structures with CT attenuation less than 150 HU were removed as the focus of this study was pulmonary arteries. Bony structures and cardiac chambers have high CT attenuation (>300 HU), thus, removal of these structures was conducted by the function of Object Separator that is available with Analyze 12.0. Some manual editing was applied to ensure the accuracy of 3D model in the delineation of pulmonary arterial tree. This involved further removal of some structures that were still included in the 3D volume data such as overlapping tissues and presence of artifacts, and applying a median filter to remove some image noise for better definition of pulmonary arteries with side branches. The generated model of the segmented pulmonary arteries was subsequently exported to the Standard Tessellation Language (STL) file format which is commonly used for 3D printing. Figure 1 shows the steps of image post-processing and segmentation from original 2D DICOM images to generation of segmented volume data and STL file to the final step of 3D printed model.

The STL file of 3D segmented pulmonary artery was uploaded to *Shapeways,* an online 3D printing service. [26] The model was printed in 'Elasto Plastic' material, which has material property closest to that of arterial wall. [27]

CTPA scanning protocols for 3D printed model

To determine the accuracy of the 3D printed model in replicating anatomical structures, a series of CTPA scans were conducted on the 3D printed pulmonary artery model with different scanning protocols. A total of nine scans were performed, in which three tube voltages of 80, 100 and 120 kVp, three pitch values of 0.7, 0.9 and 1.2 were tested. The 3D printed model was placed in a plastic box filled with a contrast medium (Omnipaque 370) (Figure 2), and scans were performed on a 64-slice CT scanner (Siemens Definition AS, Siemens Healthcare, Forchheim, Germany) with slice thickness of 1.0 mm and reconstruction interval of 0.6 mm. The contrast medium was diluted to 6% resulting in CT attenuation of 150 HU which is similar to that of clinical CTPA examination. DICOM images of the scanned model were transferred to a workstation for measurements of pulmonary artery diameters and image quality.

Measurements of pulmonary artery diameters

Diameter measurements at the pulmonary trunk, right and left main pulmonary arteries were performed on original CTPA images, STL file, 3D printed model and post-3D printing scanned CT images. Measurements were performed by two observers with more than 10 years of experience in CT imaging, with each measurement repeated three times. The two observers performed measurements separately and the results showed a very high correlation between these two observers ($r=0.99-1.0$, $p<0.001$). Figure 3 shows an example of measuring the pulmonary trunk using an electronic calliper.

Quantitative measurements of image quality

Image quality was assessed by measuring the image noise, which is defined as standard deviation (SD) of CT attenuation (HU) in the pulmonary arteries. A circular region of interest with a diameter of 50 mm^2 (containing 300 voxels within the ROI) was placed at the pulmonary trunk, left main and right main pulmonary arteries to measure the signal-to-noise ratio (SNR) which is defined as:

SNR = CT attenuation in the pulmonary artery / SD

Figure 4 is an example showing measurement of image quality (SNR) at the pulmonary trunk, left main and right main pulmonary arteries. Contrast-to-noise ratio (CNR) was not measured in this study due to lack of background tissue since 3D printed model was immersed into the contrast medium. The two observers performed measurements separately and the results showed a high correlation between these two observers ($r=0.99-1.0$, $p<0.05$).

Radiation dose

Radiation dose values in terms of volume CT dose index (CTDIvol) and dose length product (DLP) were available on the CT console. Effective dose (ED) was calculated by multiplying the DLP by a tissue coefficient factor, which is 0.014 mSv.mGy.cm for chest CT scan. [28]

Statistical analysis

Data were entered into MS Excel for analysis. Continuous variables were presented as mean ± standard deviation. A two-sided Student T test was used to determine any significant differences between measurements performed at original CT, STL, 3D printed model and post-3D printing scanned images, with p value of less than 0.05 indicating statistical significance.

RESULTS

CT scans of the 3D printed pulmonary artery model were successfully performed. Table 1 shows measurements of the main pulmonary arteries made with different scanning protocols when compared to the original CTPA images with differences less than 0.8 mm, indicating high accuracy of 3D printed model in replicating anatomical structures. There was also very good correlation between measurements on STL file in comparison to those on original CT images, post-3D printed CT images and 3D printed model, with the mean difference less than 0.5 mm.

Table 2 shows SNR measurements at different CTPA protocols with corresponding radiation dose values. With 80 and 100 kVp protocols, SNR was slightly decreased when pitch was increased from 0.7 to 0.9 and 1.2, although this did not reach significant difference in measurements with these protocols (p=0.96-0.99). With 120 kVp protocol, SNR was slightly increased with the increase of pitch in most of the measurements, with no statistical significance difference noted (p=0.97-0.99).

Table 2 also shows radiation dose values associated with these CTPA protocols. As shown in Table 2, CTDIvol and DLP remained almost the same despite the use of different pitch values, mainly due to the use of tube current modulation. With 80 kVp as the selected protocol, the effective dose was reduced by 55% and 75% when kVp was lowered from 100 and 120 kVp, respectively, while still maintaining diagnostic image quality. Figure 5 shows coronal reformatted CT images acquired with 9 different protocols with good visualisation of the pulmonary trunk and left and right main pulmonary arteries.

DISCUSSION

This preliminary study has two main findings: Firstly, 3D printed pulmonary artery model has high accuracy in replicating anatomical structures, thus it can be used as a reliable tool for testing CT scans. Secondly, an optimal CTPA protocol can be developed through testing different scanning protocols on the 3D printed model, with a protocol of 80 kVp and pitch 0.9 being the optimal one with resultant low radiation dose but maintaining diagnostic image quality.

3D printed models have been shown to enhance understanding of complexity of cardiovascular disease by demonstrating accuracy of delineating anatomical structures and pathologies, pre-operative planning and simulation, and medical education. [6-15] Case reports and case series studies have proved successful applications of 3D printed models in assisting diagnosis and clinical management of congenital heart diseases including pulmonary artery abnormalities. [29-33] A recent case report discussing the 3D printed model of ventricular septal defect (VSD) and pulmonary atresia showed that 3D printing assisted the development of preoperative planning and treatment approach for managing this complex case. [30] Sahayaraj et al further confirmed the clinical value of using 3D printed model in managing complex cardiovascular cases involving great vessels. [31] The 3D printed model was found to have great value in improving understanding of the spatial relationship between cardiac chambers, VSD and great arteries, with biventricular physiologic repair successfully performed owing to the increased spatial perception provided by the 3D printed model.

Biglino and colleagues provided an insight into the clinical applications of 3D printed heart model based on the perspective from different stakeholders. [29] The 3D printed model was considered by surgeon and cardiologist to improve understanding of the 3D relationship of different structures, such as better demonstrating the narrowed pulmonary artery and the dilated ascending aorta. Medical imaging specialist considered that 3D printed model improved communication in multidisciplinary meetings, thus allowing better decision-making in patient treatment. Further, a medical student indicated the great potential of 3D printed models in teaching anatomy and pathology. [29]

Despite promising results about the clinical value of 3D printed models, reports on the dimensional accuracy of 3D printed pulmonary artery model are scarce. Most of the current studies focus on the accuracy of 3D printed heart models, in particular, congenital heart disease with good correlation between 3D printed models and original source images. [5-9] However, in their recent study, Ho et al reported the mean difference of more than 1.0 mm in aortic vessel diameters between contrast-enhanced CT images before and after 3D printing. [34] The variance in dimensional accuracy was also demonstrated by Lau et al who showed the mean diameter difference between 3D printed model of brain tumour and original images being 0.98%, which exceeds the recommended 0.5% deviation. [35] Findings in this study showed high accuracy of the 3D printed pulmonary artery model with the mean difference less than 0.5% deviation in measurements between pre- and post-3D printing images. Thus, results of CT scans based on the 3D printed model could be used as a reliable source for determining optimal scanning protocols in terms of acquiring diagnostic images with radiation dose reduction.

Increased use of CTPA in clinical practice has raised concerns because of its associated high radiation exposure and potential risk of contrast-induced nephropathy. [16, 20] Therefore, optimisation of CTPA protocol is a hot topic in the current literature with successful reductions in both radiation dose and contrast medium dose achieved. Findings of this study are in line with these previous reports on patient's data. [16-20] Low tube voltage and low pitch value such as 80 kVp and 0.9 is preferred with acquisition of acceptable diagnostic images (similar SNR values) but low radiation dose when compared to the protocol of 100 or 120 kVp and high pitch value. The current multislice CT scanners are equipped with latest dose-reduction protocols, such as automatic tube current or tube potential modulation, therefore, high pitch is not recommended. The pitch of 0.9 as recommended by this study is consistent with Boos et al who also proposed the 70 kVp and pitch of 0.9 CTPA protocol. [36] We did not include 70 kVp in this study as 100 or 120 kVp is commonly used in CTPA. Further, due to 3D printed model being static instead of having hemodynamic flow features, we did not assess the effect of changing contrast medium volume on image quality. This could be addressed in further studies.

Despite promising results, this study has several limitations which need to be acknowledged. Firstly, the 3D printed model was based on a normal case without showing any sign of pulmonary embolism. Thus, no subjective assessment of image quality was conducted. Experiments on the optimal CTPA protocols in the detection of pulmonary embolism with use of 3D printed model are under investigation. Secondly, although the 3D printed model was made with elastic material, it still does not represent the real tissue properties of vascular wall. Further, the phantom was scanned in a static condition instead of representing realistic CTPA with blood circulating to the pulmonary arteries. Finally, due to including only one case, we did not perform Bland-Altman assessment of degree of agreement in measurements between pre- and post-3D printing images. Further studies should include more cases for generating 3D printed models, which would allow for more reliable detection of trends in bias.

CONCLUSION

We have shown the feasibility of generating patient-specific 3D printed pulmonary artery model with high accuracy in replicating normal anatomical structures. The 3D printed model is used to test different CT pulmonary angiography protocols with the protocol of 80 kVp, pitch 0.9 with 1 mm slice thickness and reconstruction interval of 0.6 mm being the optimal one. Future research based on simulation of pulmonary embolism with different CT scanning parameters is needed to determine the clinical value of 3D printed model in detection of pulmonary embolism with lower radiation dose while still maintaining diagnostic image quality.

ACKNOWLEDGEMENTS

This work was supported by The Pawsey Supercomputing Centre through the use of advanced visualisation resources located at The Australian Resources Research Centre with funding from the Australian Government and the Government of Western Australia. The authors would also like to acknowledge the assistance of Dr Lionel Esteban, Manager, NGL Medical XCT facility, CSIRO, Oil, Gas & Fuels Program in the acquisition of the CT scans of the pulmonary artery model.

Conflicts of interest: There are no conflicts of interest.

REFERENCES

1. Valverde I, Gomez G, Gonzales A, Suarez-Mejias C, Adsuar AF, et al. Three-dimensional patient-specific cardiac model for surgical planning in Nikaidoh procedure. Cardiol Young 2015;25(4):698-704.
2. Ebert J, Özkol E, Zeichner A, Uibel K, Weiss O, Koops U, et al. Direct inkjet printing of dental prostheses made of zirconia. J Dent Res 2009;88(7):673–676.
3. Ploch CC, Mansi CSSA, Jayamohan, J, Kuhl, E. Using 3D printing to create personalized brain models for neurosurgical training and preoperative planning. World Neurosurg 2016;90:668-674.
4. Martelli N, Serrano C, van den Brink H, Pineau J, Prognon P, Borget I, et al. Advantages and disadvantages of 3-dimensional printing in surgery: A systematic review. Surgery 2016;159:1485-1500.
5. Bartel T, Rivard A, Jimenez A, Mestres CA, Muller S. Medical three-dimensional printing opens up new opportunities in cardiology and cardiac surgery. Eur Heart J 2017 Feb 16. doi: 10.1093/eurheartj/ehx016. [Epub ahead of print].
6. Schmauss D, Haeberle S, Hagl C, Sodian R. Three-dimensional printing in cardiac surgery and interventional cardiology: a single-centre experience. Eur J Cardiothorac Surg 2015;47(6):1044–1052.
7. Biglino G, Koniordou D, Gasparini M, Capelli C, Leaver LK, Khambadkone S, et al. Piloting the use of patient-specific cardiac models as a novel tool to facilitate communication during clinical consultations. Pediatr Cardiol 2017;38:813-818.
8. Cantinotti M, Valverde I, Kutty S. Three-dimensional printed models in congenital heart disease. Int J Cardiovasc Imaging 2017;33:1337-144.

9. Giannopoulos AA, Mitsouras D, Yoo SJ, Liu PP, Chatzizisis YS, Rybicki FJ. Applications of 3D printing in cardiovascular diseases. Nat Rev Cardiol 2016;13:701-18.

10. Bhalta P, Tretter JT, Chikkabyrappa S, Chakravarti S, Mosca RS. Surgical planning for a complex double-outlet right ventricle using 3D printing. Echocardiography 2017;34:802-804.

11. Lim KH, Loo ZY, Goldie S, Adams J, McMenamin P. Use of 3D printed models in medical education: A randomized control trial comparing 3D prints versus cadaveric materials for learning external cardiac anatomy. Anat Sci Educ 2016;9(3):213-221.

12. Costello J, Olivieri L, Krieger A, Thabit O, Marshall MB, Yoo SJ, et al. Utilizing three-dimensional printing technology to assess the feasibility of high-fidelity synthetic ventricular septal defect models for simulation in medical education. World J Pediatr Congenit Heart Surg 2014;5(3):421-426.

13. Costello JP, Olivieri LJ, Su L, Krieger A, Alfares F, Thabit O, et al. Incorporating three-dimensional printing into a simulation-based congenital heart disease and critical care training curriculum for resident physicians. Congenit Heart Dis 2015;10(2):185–190.

14. Sun Z, Lee SY. A systematic review of 3-D printing in cardiovascular and cerebrovascular diseases. Anatol J Cardiol 2017 2017;17:423-35.

15. Giannopoulos AA, Steigner ML, George E, Barlie M, Hunssaker AR, Rybicki FJ, Mitsouras D. Cardiothoracic applications of 3-dimensional printing. J Thorac Imaging 2016:31:253-72.

16. Mayo J, Thakur Y. Pulmonary CT angiography as first-line imaging for PE: image quality and radiation dose considerations. AJR Am J Roentgenol 2013; 200(3): 522–528.

17. Wittram C. How I do it: CT pulmonary angiography. AJR Am J Roentgenol 2007;188(5): 1255–1261.
18. den Exter AL, van der Hulle T, Klok FA, Huisman MV. Advances in the diagnosis and management of acute pulmonary embolism. Thromb Res 2014;133(Suppl 2): S10-16.
19. Righini M, Le GG, Aujesky D, Roy RM, Sanchez O, Verschuren F, et al. Diagnosis of pulmonary embolism by multidetector CT alone or combined with venous ultrasonography of the leg: a randomised non-inferiority trial. Lancet 2008;371(9621): 1343-52.
20. Sun Z, Lei J. Diagnostic yield of CT pulmonary angiography in the diagnosis of pulmonary embolism: a single center experience. Interv Cardiol 2017;9: 191-198.
21. Ong CW, Malipatil V, Lavercombe M, Teo KGW, Coughlin PB, Leach D, et al. Implementation of a clinical prediction tool for pulmonary embolism diagnosis in a tertiary teaching hospital reduces the number of computed tomography pulmonary angiograms performed. Intern Med J 2013;43:169-74.
22. Newman DH, Schriger DL. Rethinking testing for pulmonary embolism: less is more. Ann Emerg Med 2011; 57:622-7.e3.
23. Mitsouras D, Liacouras P, Imanzadeh A, Giannopolous AA, Cai T, Kumamaru KK, George E, Wake N, Caterson EJ, Pomahac B, Ho VB, Grant GT, Rybicki FJ. Medical 3D printing for the radiologist. Radiographics 2015; 35(7):1965-1988.
24. Madurska MJ, Poyade M, Eason D, Rea P, Watson AJM. Development of a patient-specific 3D-printed liver model for preoperative planning. Surg Innov 2017; 24(2):145-150.
25. Witowski JS, Coles-Black J, Zuzak TZ, Pedziwiatr M, Chuen J, Major P, Budzynki A. 3D printing in liver surgery: A systematic review. Telemed J E Health 2017; 23(12):1-5.

26. Shapeways. Frequently Asked Questions. Available from: http://www.shapeways.com/support/faq?li=footer#faq-whatisshapeways.

27. https://www.shapeways.com/materials/elasto-plastic

28. McCollough CH, Primak AN, Braun N, Kofler J, Yu L, Christner J. Strategies for reducing radiation dose in CT. Radiol Clin North Am 2009; 47: 27 –40.

29. Biglino G, Moharem-Elgamal S, Lee M, Tulloh R, Caputo M. The perception of a three-dimensional-printed heart model from the perspective of different stakeholders: A complex case of truncus ateriosus. Front Pediatr 2017;5:209.

30. Jaworski R, Haponiuk I, Chojnicki M, Olszewski H, Lulewicz P. Three-dimensional printing technology supports surgery planning in patients with complex con-genital heart defects. Kardiol Pol 2017;75:185.

31. Sahayaraj RA, Ramanan S, Subramanyan R, Cherian KM. 3D printing to model surgical repair of complex congenitally corrected transposition of the great arteries. World J Pediatr Congenit Heart Surg 2017; Jan 1:2150135117704655. doi: 10.1177/2150135117704655. [Epub ahead of print].

32. Jones TW, Seckeler MD. Use of 3D models of vascular rings and slings to improve resident education. Congenit Heart Dis 2017;12:578-582.

33. Kappanayil M, Koneti NR, Kannan RR, Kottavil BP, Kumar K. Three- dimensional-printed cardiac prototypes aid surgical decision-making and preoperative planning in selected cases of complex congenital heart diseases: early experience and proof of concept in a resource-limited environment. Ann Pediatr Cardiol 2017:10:117–25.

34. Ho D, Squelch A, Sun Z. Modeling of aortic aneurysm and aortic dissection through 3D printing. J Med Radiat Sci 2017;64:10-17.

35. Lau I, Squelch A, Wan YL, Wong A, Ducke W, Sun Z. Patient-specific 3D printed model in delineating brain glioma and surrounding structures in a pediatric patient. Digit Med 2017;3:86-92.

36. Boos J, Kropil P, Lanzman RS, Aissa J, Schleich C, Heusch P, et al. CT pulmonary angiography: simultaneous low-pitch dual-source acquisition mode with 70 kVp and 40 ml of contrast medium and comparison with high-pitch spiral dual-source acquisition with automated tube potential selection. Br J Radiol 2016;89:20151059.

Figure legends

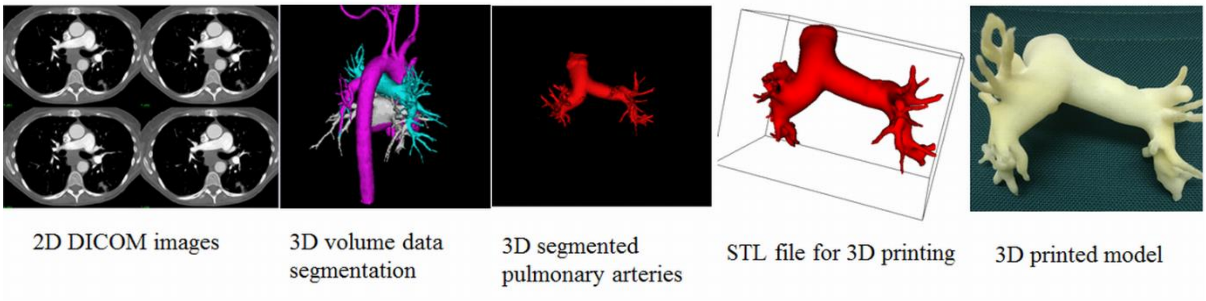

Figure 1. Flow diagram shows the image post-processing and segmentation steps from 2D CT images to creation of 3D printed model. Original 2D DICOM (Digital Imaging and Communications in Medicine) images were used to create 3D volume rendering image with use of CT number thresholding technique to display contrast-enhanced vessels (blue colour-pulmonary arteries, pink colour-aorta and its branches, while colour-left atrium and pulmonary veins). 3D volume rendering of pulmonary artery tree is segmented through semi-automatic segmentation and manual editing. STL (Standard Tessellation Language) file of 3D segmented volume data was generated for 3D printing of patient-specific 3D printed model.

Figure 2. 3D printed pulmonary model is placed in a plastic box which is used to be filled with contrast medium for CT scans.

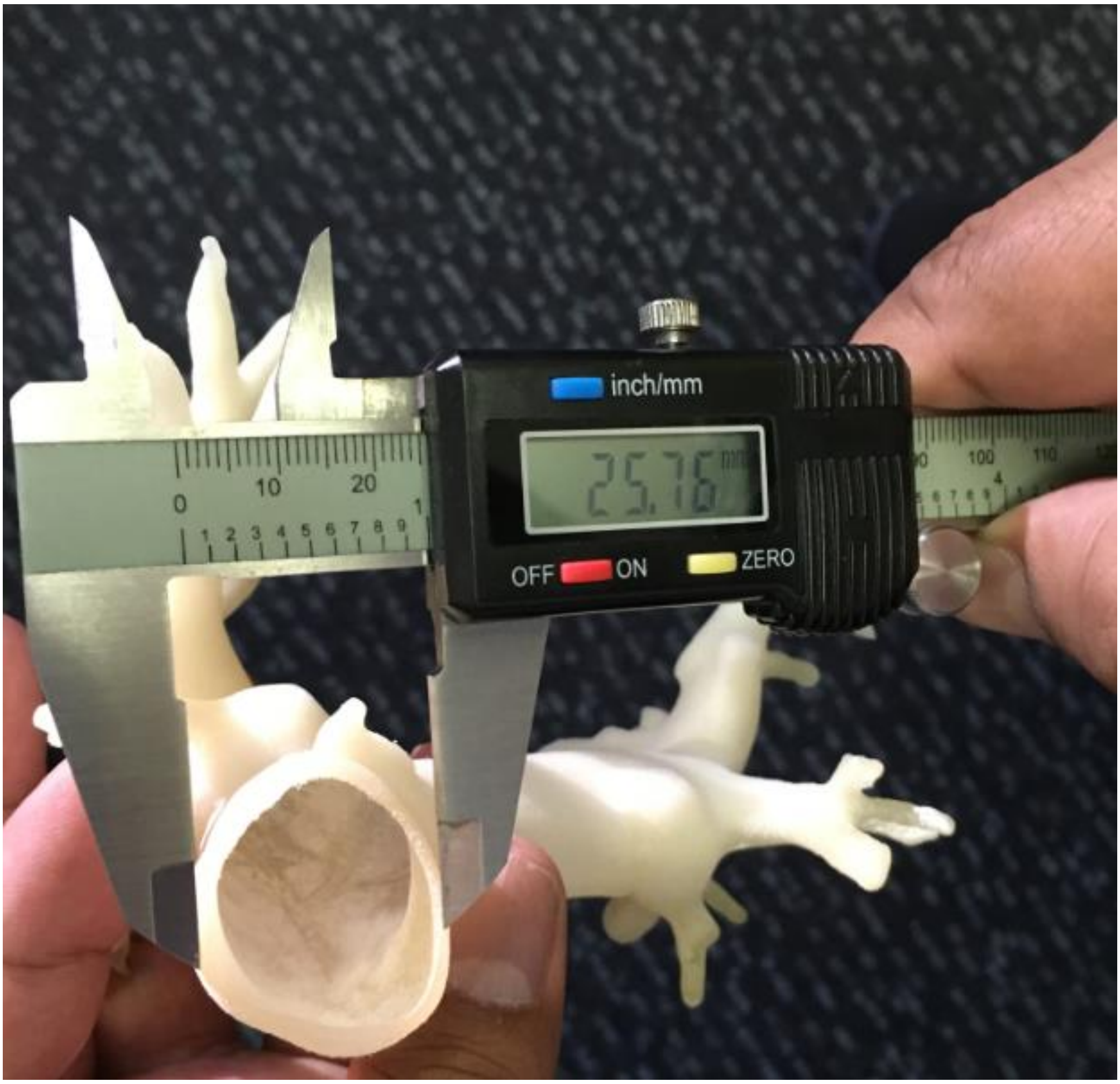

Figure 3. Measurement of the diameter of a pulmonary trunk using an electronic calliper.

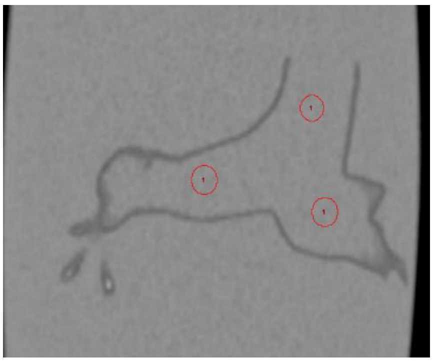

Figure 4. Region of interest is placed at the pulmonary trunk, right and left main pulmonary arteries for measurement of image quality.

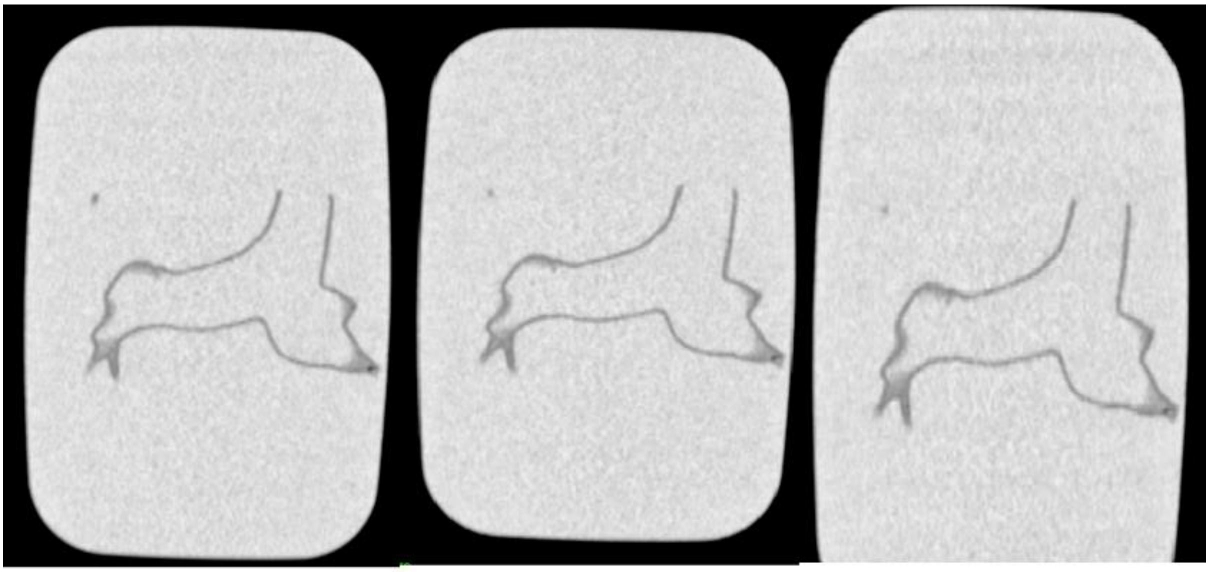

80 kVp with pitch 0.7 | 80 kVp with pitch 0.9 | 80 kVp with pitch 1.2

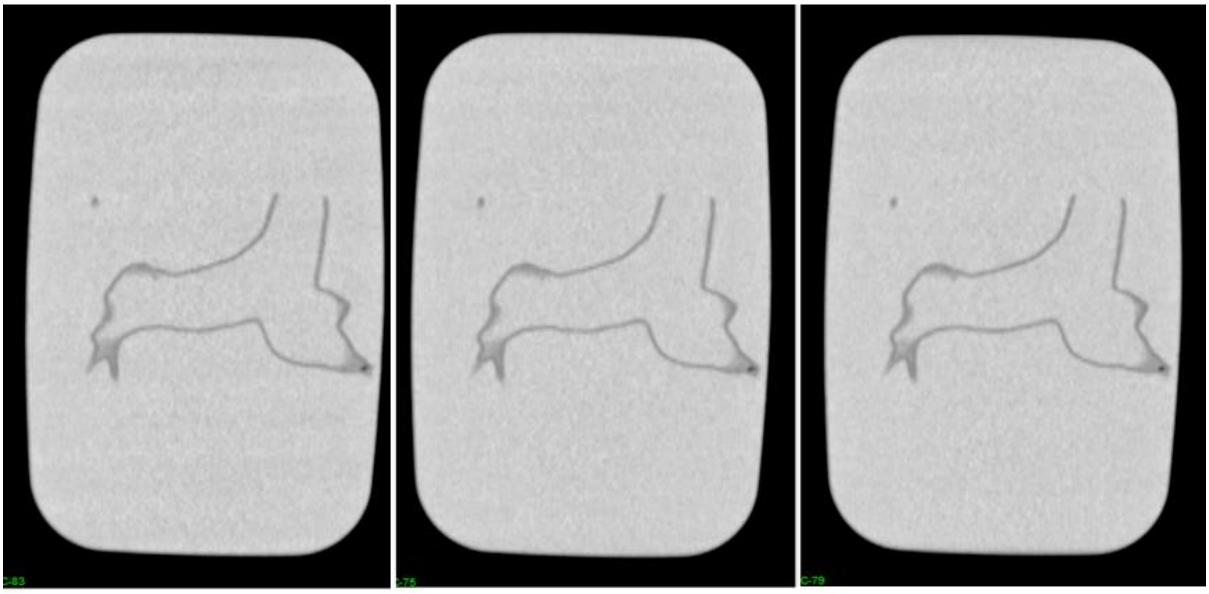

100 kVp with pitch 0.7 | 100 kVp with pitch 0.9 | 100 kVp with pitch 1.2

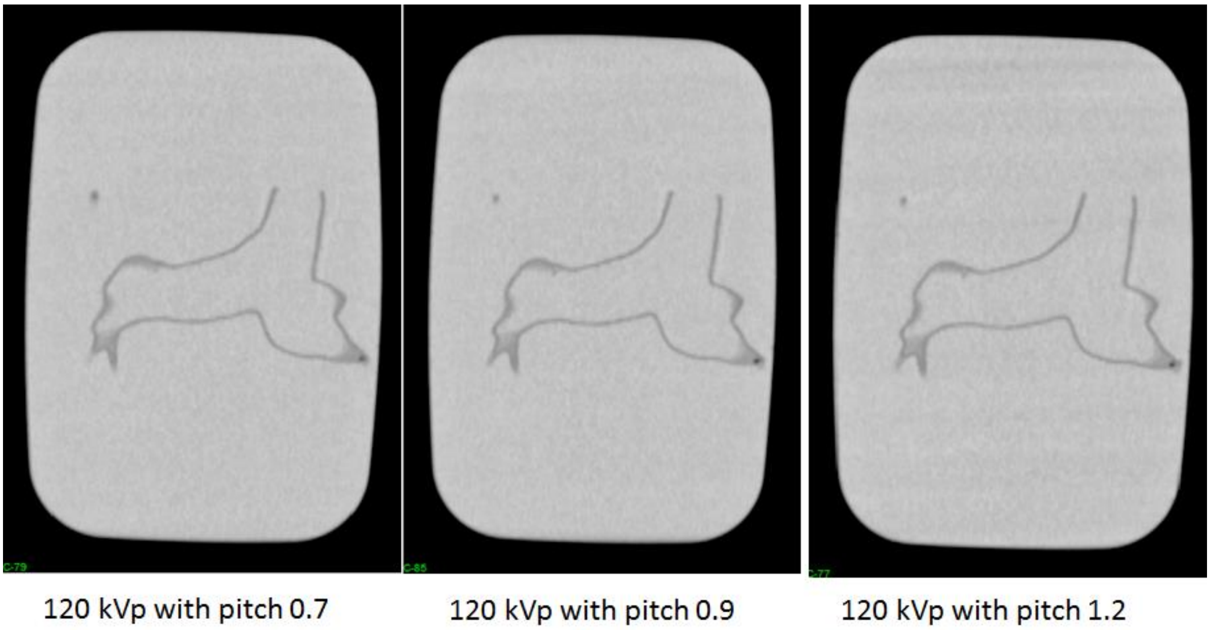

Figure 5. CT pulmonary angiography scanning protocols in the 3D printed model. 2D coronal reformatted images showing main pulmonary trunk, right and left main pulmonary arteries with 80 kVp, pitch 0.7, 0.9 and 1.2 (A), 100 kVp, pitch 0.7, 0.9 and 1.2 (B), 120 kVp, pitch 0.7, 0.9 and 1.2 (C).

Table 1. Diameters of pulmonary arteries measured on CT scanned 3D printed model

Measurement locations	**80 kVp protocol (mean mm)**			**100 kVp protocol (mean mm)**			**120 kVp protocol (mean mm)**		
	Pitch 0.7	**Pitch 0.9**	**Pitch 1.2**	**Pitch 0.7**	**Pitch 0.9**	**Pitch 1.2**	**Pitch 0.7**	**Pitch 0.9**	**Pitch 1.2**
Pulmonary trunk	25.44	25.97	25.59	25.77	25.13	25.1	25.97	25.86	25.94
Left pulmonary artery	26.57	26.11	26.88	26.25	26.72	26.31	26.22	26.79	26.86
Right pulmonary artery	21.77	21.88	21.45	21.66	21.07	21.41	21.23	21.23	21.45
Original CT images	Pulmonary trunk: 25.93, LPA: 26.20, RPA: 21.63								
STL images	Pulmonary trunk: 25.98, LPA: 26.03, RPA: 21.90								
3D printed model	Pulmonary trunk: 25.85, LPA: 26.02, RPA: 21.84								

LPA-left pulmonary artery, RPA-right pulmonary artery, STL-standard tessellation language

Table 2. Quantitative measurement of image quality and radiation dose in different CT scanning protocols

Measurement locations	**80 kVp protocol**			**100 kVp protocol**			**120 kVp protocol**		
	Pitch 0.7	**Pitch 0.9**	**Pitch 1.2**	**Pitch 0.7**	**Pitch 0.9**	**Pitch 1.2**	**Pitch 0.7**	**Pitch 0.9**	**Pitch 1.2**
SNR at pulmonary trunk	13.28	12.79	11.41	20.29	14.68	13.36	17.18	19.46	18.99
SNR at left main pulmonary artery	13.44	12.16	10.59	14.81	14.73	10.97	14.18	16.28	16.27
SNR at right main pulmonary artery	10.25	10.84	10.08	15.11	10.97	11.19	15.21	17.35	15.72
CTDIvol (mGy)	5.81	5.73	5.62	12.96	12.84	12.64	23.12	22.90	22.61
DLP (mGy.cm)	128	128	128	286	286	286	510	511	514
ED (mSv)	1.79	1.79	1.79	4.04	4.04	4.04	7.14	7.15	7.19